2014 5th IEEE RAS & EMBS International Conference on
Biomedical Robotics and Biomechatronics (BioRob)
August 12-15, 2014. São Paulo, Brazil

Electromagnetic Actuation System for Locomotive Intravascular Therapeutic Microrobot

Hyunchul Choi, Gwangjun Go, Cheong Lee, Seong Young Ko, Semi Jeong, Kiduk Kwon, Jong-Oh Park* and Sukho Park*, *Member, IEEE*

Abstract— **In this paper, we proposed an intravascular therapeutic microrobot using an electromagnetic actuation (EMA) system with bi-plane X-ray imaging device. The proposed EMA system consists of Helmholtz-Maxwell coils, uniform-gradient saddle coils. The Helmholtz-Maxwell coils are located along y-axis, and uniform-gradient saddle coils are located perpendicular to y-axis. In order to align the microrobot along a desired angle in 2D (dimensional) plane, it is necessary to control of the currents on Helmholtz coil and uniform saddle coil. For a forward and backward direction movement of the microrobot, we precisely control the currents of Maxwell coil and gradient saddle coil. Because the saddle coils can be rotated around the y-axis, the effective actuation plane of the microrobot can be also rotated, and the microrobot can move in 3D space. In addition, for the position recognition of the microrobot in a blood vessel, we adopted a bi-plane X-ray fluoroscopy. If the saddle coils are rotated around the y-axis, an open area is changed. Therefore, the saddle coils and bi-plane X-ray fluoroscopy must be rotated simultaneously. To confirm the feasibility of 3D locomotion of the microrobot, we executed a locomotion test of the microrobot in the blood vessel phantom, where the blood vessel phantom was fabricated by the rendering data from computed tomography (CT) images of the iliac artery and 3D printer.**

I. Introduction

RECENTLY, in order to targeted drug delivery and therapy of the disease, many researchers developed manipulation method of magnetic nano particle (MNP) containing the beads and microrobot [1-12].

Because size limitation of the microrobot, the power source and motor are difficult to integrate into the microrobot. Therefore, many wireless microrobots actuated by external magnetic field (electromagnet, permanent magnet).

First, for the actuation of the microrobot in blood vessel, researchers need study about microrobot design and fabrication method for suitable purpose (DDS, therapy) [4-6]. In addition, research is needed on the EMA system for manipulation of the microrobot in the blood vessel. Lastly, important issue is detection of the orientation and position of the microrobot.

Many researchers developed the EMA system integrated with imaging devices. But, most researches are conducted the observation of the microrobot using CCD camera [7-10]. However, if the microrobot inserted into the blood vessel, this method is difficult to observe. S. Martel proposed the magnetic field generated by a conventional MRI system to drive a microbead [11-12]. The MRI system can manipulate the microbead and recognize its position, simultaneously. However, the MRI based microbead manipulation system cannot have a sufficient force for the locomotion in the blood vessels.

In this paper, we propose intravascular therapeutic microrobot system with 3D locomotion and detection. The EMA system consist Helmholtz-Maxwell coils, uniform-gradient saddle coils. For the detection of the microrobot, the EMA system is integrated with bi-plane X-ray fluoroscopy.

II. Electro Magnetic Actuation System

A. Basic Theory

Magnetic torque and force applied to a magnetic materials in a magnetic field can be derived by the following equations [10, 13]:

$$\mathbf{T} = \mu_0 V \mathbf{M} \times \mathbf{H} \tag{1}$$

$$\mathbf{F} = \mu_0 V (\mathbf{M} \cdot \nabla) \mathbf{H} \tag{2}$$

where $\mathbf{T}$, V, $\mathbf{M}$, and $\mathbf{B}$ are the torque, the volume of magnetic material, and the magnetization vector of the microrobot, magnetic flux, respectively. In addition, ∇ is the gradient operator. From Eq. (1) and (2), the torque and force, which are generated by a microrobot composed of permanent magnet, can be calculate, where it surrounded by magnetic field.

The Helmholtz coil and uniform saddle coil are generate a uniform magnetic field in ROI. And the magnetic fields,

* This research was supported by the Industrial Strategic Technology Development Program (10030037, CTO Therapeutic System) funded by the Ministry of Trade. Industry and Energy (MOTIE, Korea), and by Leading Foreign Research Institute Recruitment Program (No. 2012-026740) through the National Research Foundation of Korea (NRF) funded by the Ministry of Education, Science and Technology (MEST, Korea).

Hyunchul Choi, Gwangjun Go, Cheong Lee, and Seong Young Ko are with the School of Mechanical Engineering, Chonnam National University, Gwangju, 500-757, Korea (e-mail: hichc @nate.com, gwangjun124@gmail.com, vdkqydh@naver.com, and sko@jnu.ac.kr)

Semi Jeong and Kiduk Kwon are with Robot Research Initiative, Chonnam National University, Gwangju, 500-757, Korea (e-mail: semi@jnu.ac.kr and kdkwon@jnu.ac.kr).

Jong-Oh Park and Sukho Park are with School of Mechanical Systems Engineering, Chonnam National University, Gwangju 500-757, Korea (corresponding author phone: 82-62-530-1687; fax: 82-62-530-0267; e-mail: jop@jnu.ac.kr and spark@jnu.ac.kr).

which are generated by each coil assembly, are derived as follows:

$$\mathbf{H}_{\boldsymbol{h}} = \begin{bmatrix} 0 & \frac{0.7155 \times n_h \times i_h}{r_h} & 0 \end{bmatrix}^T \quad (3)$$

$$\mathbf{H}_{\boldsymbol{us}} = \begin{bmatrix} 0 & \frac{0.6004 \times n_{us} \times i_{us}}{r_{us}} & 0 \end{bmatrix}^T \quad (4)$$

where i_h, n_h and r_h are the input current, turns and radius of the Helmholtz coil, i_{us}, n_{us} and r_{us} are the input current, turns and radius of the uniform saddle coil.

The Maxwell coil and gradient saddle coil are generate a uniform gradient magnetic field in ROI. And the magnetic field, which are generated by each coil assembly, are derived as follows:

$$\mathbf{H}_{\boldsymbol{m}} = [-0.5 g_m x \quad g_m y \quad -0.5 g_m z]^T \quad (5)$$

$$\mathbf{H}_{\boldsymbol{gs}} = [-1.4398 g_{gs} x \quad -g_{gs} y \quad 2.4398 g_{gs} z]^T \quad (6)$$

where the gradient of Maxwell coils (g_m) and gradient saddle coil (g_{gs}) are derived as follows:

$$g_m = 0.6413 \times \frac{i_m \times n_m}{{r_m}^2} \quad (7)$$

$$g_m = 0.3286 \times \frac{i_{gs} \times n_{gs}}{{r_{gs}}^2} \quad (8)$$

where i_m, n_m and r_m are the input current, turns and radius of the Maxwell coil, and i_{gs}, n_{gs} and r_{gs} are the input current, turns and radius of the gradient saddle coil.

B. Actuation Mechanism

Previously, we proposed an EMA system, which is comprised of 1-pair of Helmholtz-Maxwell coils, and 1-pair of uniform- gradient saddle coils. And the saddle coils are rotate on axis of Helmholtz-Maxwell coils [10]. This system, as shown in Fig. 1, can align the microrobot to desired direction by controlling of input current for Helmholtz coil and uniform saddle coil. And the system can move the microrobot to aligned direction with desired magnitude by controlling of input current for Maxwell coil and Gradient saddle coil. Additionally, by rotating of working plane which were made by saddle coil assembly, the working area is expandable for 3-D locomotion.

Firstly, the input current of Helmholtz coils and uniform saddle coil for alignment of the microrobot to desired direction with θ, is derived as follows:

$$i_{us} = 1.1917 \times \tan\theta \times \frac{r_{us} \times n_h}{r_h \times n_{us}} \times i_h \quad (9)$$

In sequence, the input current of Maxwell coils and gradient saddle coil for movement of microrobot to aligned direction, is derived as follows:

$$i_m = 1.1717 \times \left(\frac{r_m}{r_{gs}}\right)^2 \times \frac{n_{gs}}{n_m} \times i_{gs} \quad (10)$$

TABLE I
SPECIFICATION OF EMA SYSTEM

	HC	MC	USC	GSC
Radius (mm)	195	195	141	141
Turns	556	1143	448	448
Resistance (Ω)	14.43	25.69	30.45	17.6
Uniform field (1A, A/m)	2040		1908	
Field gradient (1A, A/m^2)		19277		7405

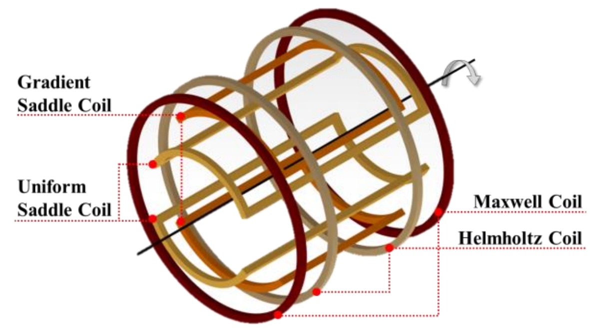

(a) Isotropic view

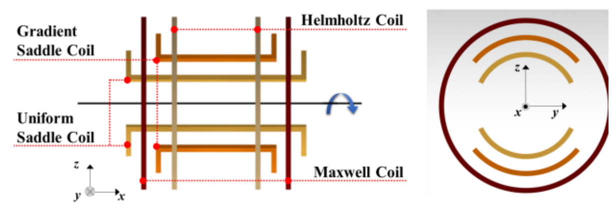

(b) Front and side view

Fig. 1. Schematic diagram of the coil system.

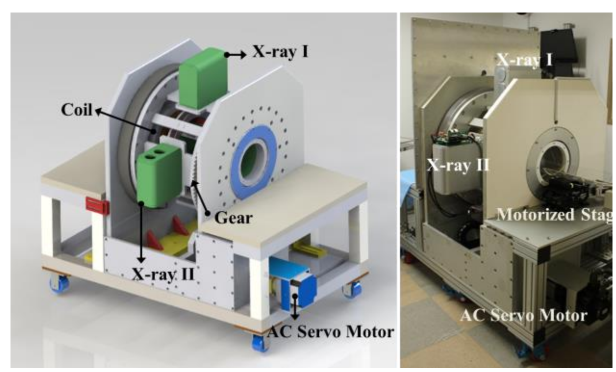

Fig. 2. Design and fabrication of the EMA system with bi-plane X-ray fluoroscope system (ViVIX, Vatech korea).

Lastly, in order to move on plane, which is tilted with Φ, the compensation of gravity for tangential direction is necessary. For this, the gradient, which is generated by the Maxwell coil and gradient saddle coil, is derived as follows:

$$g_{gs} = \frac{mg \sin\emptyset}{3.4398 \times M \times V \times \sin\theta} - 0.3461 \times g_m \quad (11)$$

where $\emptyset$, mg, M and V are tilting angle of working plane, weight, magnetization and volume of the microrobot.

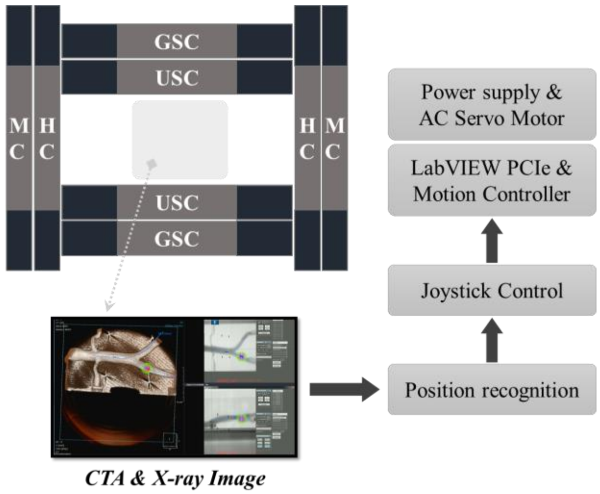

Fig. 3. Experimental setup.

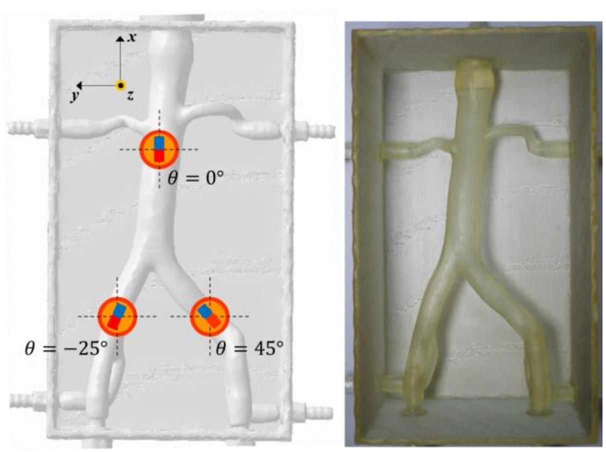

Fig. 4. Blood vessel phantom.

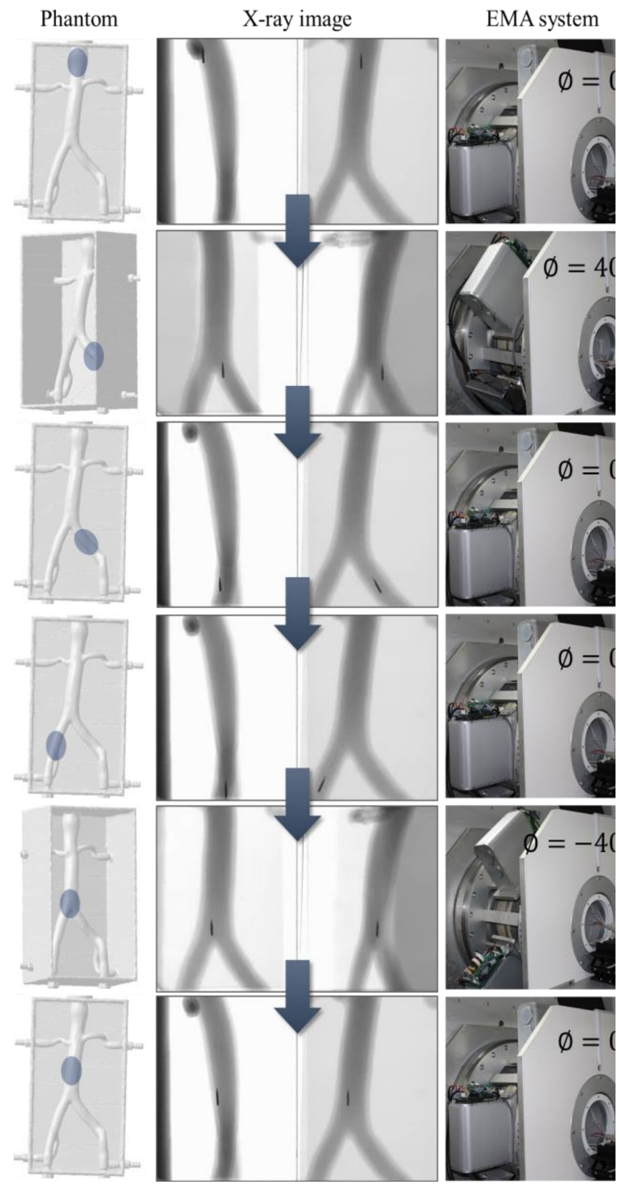

III. Experiments

A. Experimental Setup

The experimental setup is shown as Figs. 2, 3 and specification of EMA system is shown as Table 1. At the first, 3-D shape of the blood vessel image was extracted by using CT. Based on its image, the phantom with blood vessel model was fabricated through 3D print (see Fig. 4). To observe the blood vessel and create the similar environment like the real blood, interior of the phantom was filled with the physiological saline including X-ray contrast medium.

In addition, a pointy cylindrical type NdFeB magnet with 1mm diameter and 10mm length was inserted into the phantom. The motorized stage using a step motor was adopted to place the phantom in the ROI.

The current values were applied to the proposed EMA system through four power suppliers (California Instruments MX15 & 3001iX). Also, PCIe controller with LabVIEW 2010 (National Instruments) software was used to control AC servo motor and power suppliers.

B. In-vitro Test

To verify 3D locomotion of the proposed system, moving path of the microrobot had 25°, 45° in the plane, and about 10° in the inclined plane (see Fig. 4). For the movement of the microrobot in this path, the microrobot maintained the orientation along $\Phi = 0°$ (plane) and $\Phi = 45°$ (inclined plane). Specifically, to move along the inclined plane, the working plane generated by the rotating coils coincides with the inclined plane. And, the proper current values for each coils were controlled by using gravity compensation algorithm.

The alignment and propulsion of the microrobot in the 3D blood vessel model is shown as fig. 5. We confirmed that it is possible not only to observe the orientation and position of the microrobot and the moving path in the blood vessel model but also move the microrobot in the 3D space.

IV. Conclusion

In this paper, we proposed the locomotion of a microrobot in the blood vessel using stationary Helmholtz-Maxwell coils, rotational uniform-gradient saddle coils. For the orientation and position recognition of the microrobot, real time images of the microrobot were recorded by the bi-plane X-ray fluoroscopy. For 3D locomotion of the microrobot, the working plane should be rotated by the rotational uniform-gradient saddle coils. In addition, the bi-plane X-ray fluoroscopy can be rotated together with the rotational uniform-gradient saddle coil pairs. Therefore, we designed and fabricated the EMA system with the bi-plane X-ray fluoroscopy and result of the locomotion (for-backward and steering) of microrobot in the blood vessel phantom verified the feasibility. Consequently, it is expected that the proposed EMA system would have potential for use in many medical applications such as the intravascular therapeutic microrobot, in specific drug delivery and in sensor delivery, etc.

References

[1] B. J. Nelson, I. K. Kaliakatsos and J. J. Abbott, "Microrobots for minimally Invasive medicine," Annual Review of Biomedical Engineering, Vol. 12, pp. 55-85, 2010.

[2] J. J. Abbott, Z. Nagy, F. Beyeler and B. J. Nelson, "Robotics in the small-part I: microrobotics," IEEE Robotics and Automation Magazine, Vol. 14, No. 2, pp. 92-103, 2007.

[3] JianFeng, Sung Kwon Cho, "Mini and micro propulsion for medical swimmers," micromachines, Vol 5, pp. 97-113, 2014.

[4] Sangwon Kim, Famin Qiu, Samhwan Kim, Ali Ghanbari, Cheil Moon, Li Zhang, Bradley J. Nelson, and Hongsoo Choi, "Fabrication and characterization of magnetic microrobots for three-dimensional cell culture and targeted transportation," Advanced Materials, Vol. 108, No. 1, pp. 5863-5868, 2013.

[5] Shang-Hsiu Hu, Ting-Yu Liu, Dean-Mo Liu, and San-Yuan Chen, "Controlled pulsatile drug release from a ferrogel by a high-frequency magnetic field," Macromolecules, Vol. 40, pp. 6786-6788, 2007.

[6] K. Ishiyama, K. I. Aral, M. Sendoh, and A. Yamazaki, "Spiral-type micro-machine for medical applications," International Symposium on Micromechatronics and Human Science, pp. 65-69, 2000.

[7] J. Choi, S. Jeong, K. Cha, L. Qin, J. Li, B. Kim, J. Park and S. Park, "Position stabilization of microrobot using pressure signal in pulsating flow of blood vessel," IEEE Sensors, pp. 723-726, 2010.

[8] S. Jeon, G. Jang, H. Choi, and S. Park, "Magnetic navigation system with gradient and uniform saddle coils for the wireless manipulation of micro-robots in human blood vessels," IEEE Transaction on magnetics, Vol. 46, No. 6, pp. 1943-1946, 2010.

[9] S. Jeong, H. Choi, J. Choi, C. Yu, J. Park and S. Park, "Novel electromagnetic actuation (EMA) method for 3-dimensional locomotion of intravascular microrobot," Sensors and Actuators, Vol. 157, No. 1, pp. 118-125, 2010.

[10] H. Choi, K. Cha, J. Choi, S. Jeong, S. Jeon, G. Jang, J. Park and S. Park, "EMA system with gradient and uniform saddle coils for 3D locomotion of microrobot," Sensors and Actuators, Vol. 163, No. 1, pp. 410-417, 2010.

[11] J. B. Mathieu, S. Martel, Y. G. Soulez, and G. Beaudoin, "Preliminary investigation of the feasibility of magnetic propulsion for future microdevices in blood vessel," Bio-medical Materials and Engineering, Vol. 5, No. 5, pp. 367-374, 2005.

[12] S. Tammz, R. Gourdeau, A. Chanu, J.B. Mathieu, S. Martel, "Real-time MRI-based control of a ferromagnetic core for endovascular navigation," IEEE Transaction on Biomedical Engineering, Vol. 55, pp. 1854–1863, 2008.

[13] S. T. Lin and A. R. Kaufmann, "Helmholtz coils for production of powerful and uniform fields and gradients," Reviews of modern physics, Vol. 25, No. 1, pp. 182-190, 1953.